Proceedings of the 42th "Jaszowiec" International School and Conference on the Physics of Semiconductors, Wisła 2013

Electrical Properties of SbSI/Sb_2S_3 Single and Double Heterostructures

B. Toroń, M. Nowak, A. Grabowski and M. Kępińska
Solid State Physics Section, Institute of Physics, Silesian University of Technology
Z. Krasińskiego 8, 40-019 Katowice, Poland

The SbSI/Sb_2S_3 single heterostructures as well as Sb_2S_3/SbSI/Sb_2S_3 and SbSI/Sb_2S_3/SbSI double heterostructures have been produced by applying CO_2 laser treatment of *p*-type SbSI single crystals. The current–voltage and transient characteristics of these heterostructures have been measured in temperatures below and above the SbSI single crystal Curie temperature ($T_c = 293$ K). The results have been fitted with appropriate theoretical formulae to determine the following types of the investigated heterojunctions: *P–p* SbSI/Sb_2S_3, *p–P–p* Sb_2S_3/SbSI/Sb_2S_3 and *P–p–P* SbSI/Sb_2S_3/SbSI. Influence of the illumination on electrical properties of SbSI/Sb_2S_3 single and double heterostructures has been reported. Fabricated new structures may be potentially applicable in electronics and optoelectronics as a new type of metal–ferroelectric–semiconductor devices.

DOI: 10.12693/APhysPolA.124.830
PACS: 74.78.Fk, 79.60.Jv, 73.40.−c, 78.66.−w

1. Introduction

The antimony sulfoiodide (SbSI) single crystals are ferroelectric semiconductors having many useful properties. Among them, there are pyroelectric, pyrooptic, electrooptic and photoferroelectric effects. The crystalline SbSI has a chain structure and is one of the best piezoelectric crystals with high volume piezoelectric modulus $d_v = 1 \times 10^{-9}$ C/N and extremely high electromechanical coupling coefficient $k_{33} = 0.90$. The main properties of SbSI have been reviewed in a few monographs [1–3]. However, the properties of this material are still investigated [4, 5].

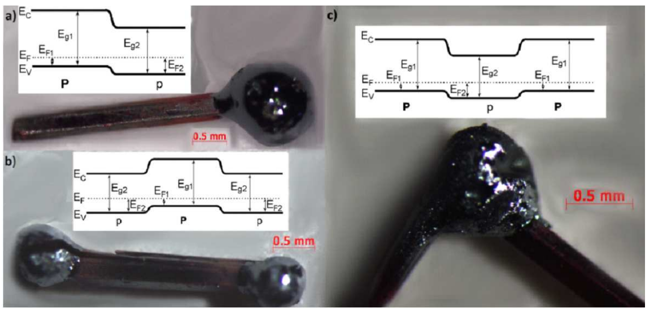

Fig. 1. Photographs of single SbSI/Sb_2S_3 heterojunction (a) as well as double Sb_2S_3/SbSI/Sb_2S_3 (b), and SbSI/Sb_2S_3/SbSI (c) heterostructures. Insets present schemes of the junction heterostructures with a band edges alignment and Fermi level position at $T = 288$ K ($E_{g1} = 1.85$ eV; $E_{F1} = 0.62$ eV; $E_{g2} = 1.62$ eV; $E_{F2} = 0.66$ eV; indices 1 and to 2 correspond to SbSI and Sb_2S_3, respectively).

Recently a new type of heterostructures has been produced in SbSI single crystals [6]. The SbSI/Sb_2S_3 heterojunctions (Fig. 1) have been fabricated by CO_2 laser irradiation of selected sections of SbSI single crystals. This irradiation evokes melting and chemical decomposition of SbSI. Laser treated sections of SbSI are composed of amorphous antimony(III) sulphide (Sb_2S_3) with energy gap 0.3 eV smaller (in room temperature) than that of SbSI [6]. Optical properties of the SbSI/Sb_2S_3 heterostructures and results of their investigations using scanning electron microscopy, energy-dispersive X-ray spectroscopy, and X-ray diffractometry have been presented in [6]. In this paper electrical properties of SbSI/Sb_2S_3, SbSI/Sb_2S_3/SbSI and Sb_2S_3/SbSI/Sb_2S_3 heterostructures are reported.

2. Experimental details

The technology of sample preparation was the same as the described in [6]. The DC current–voltage characteristics of the fabricated SbSI/Sb_2S_3 heterostructures have been determined at various temperatures using the vacuum optical D2209 chamber equipped with R2205 Cryogenic Microminiature Refrigeration II–B System and K20 temperature controller (MMR Technologies, Inc.). Vacuum ($p = 10^{-4}$ mbar) has been obtained by TSH 071E turbomolecular drag pumping station (Pfeiffer). The Keithley 6517 A electrometer has been used as the bias source. The sample has been illuminated by cw laser diode to determine the influence of illumination on electrical properties of SbSI/Sb_2S_3 heterostructures. Measurements have been performed below and above SbSI single crystal Curie temperature ($T_c = 293$ K).

3. Results and discussion

Figures 2 and 3 present DC current–voltage (I–U) characteristics of SbSI/Sb_2S_3 single heterojunction. The sample is polarized in forward direction when higher potential is applied to Sb_2S_3 part of the heterostructure. An important parameter, the ideality factor (n) that describes the ratio of recombination and diffusive currents in a junction, can be determined from I–U characteristics of heterostructures by fitting appropriate exponential dependence [7–9]:

$$I = I_0 \left[\exp\left(\frac{qU}{nkT} \right) - 1 \right], \tag{1}$$

where I is the measured current, I_0 is the preexponential constant, q is the electron charge, U is applied voltage, k is the Boltzmann constant, and T is the temperature. Solid curve in Fig. 2 presents the fitted theoretical dependence (1). The evaluated value of $n = 207(74)$ is relatively high. It might be caused by the crystalline-amorphous junction type, properties of the junction materials, as well as by inhomogeneity of the investigated junction [10]. The minimum values of the ideality factor for both non-illuminated and illuminated SbSI/Sb_2S_3 junction is observed at temperature $T = 293$ K, i.e. at the Curie point of SbSI.

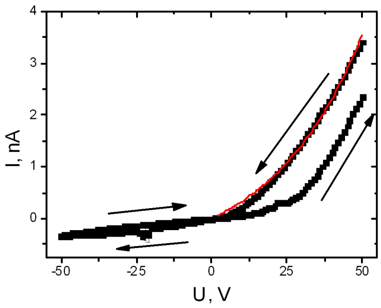

Fig. 2. Typical DC current–voltage characteristics of SbSI/Sb_2S_3 heterojunction (points) recorded at temperature $T = 263$ K with visible ferroelectric effects. Solid curve presents the fitted theoretical dependence (1). Arrows show directions of bias changes.

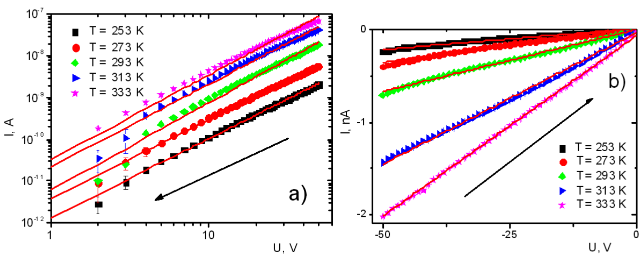

Fig. 3. Typical DC current–voltage characteristics of SbSI/Sb_2S_3 heterojunction for forward (a) and reverse polarization (b) measured (points) at different temperatures. Solid curves present the fitted theoretical dependence (2). Arrows show directions of bias changes.

Below T_c displacement of I–U characteristics has been observed (Fig. 2) due to initial poling by a DC voltage. This initial polarity determines direction of internal polarization of the SbSI. Namely, I at a given U is larger for decreasing than for increasing the voltage. Similar effect has been observed in ferroelectric (Pb,La)(Zr,Ti)O_3/$SrTiO_3$:Nb diodes [10]. The influence of SbSI ferroelectric phase on I–U characteristics of SbSI/Sb_2S_3 heterostructures can also be recognized in noticeable discontinuities appearing at $U = \pm 25$ V after repolarization (Fig. 2). These discontinuities correspond to coercive field in crystalline SbSI ($E_c = 10$ kV/m [11]). This effect disappears in temperatures greater than the Curie temperature of SbSI.

To determine the type of SbSI/Sb_2S_3 heterojunctions, the I–U characteristics have also been fitted (Fig. 3) with power function [12]:

$$I = aU^m, \tag{2}$$

where a is proportionality factor. The exponent m should have a value approximately 2 for isotype (p–p or n–n) heterojunctions or greater than 2 for anisotype (p–n) heterojunctions [12]. Fittings the forward part of I–U characteristics of SbSI/Sb_2S_3 heterojunctions with formula (2) have given values of m from 1.91(4) to 2.04(5) in the temperature range from 253 K to 333 K. Therefore, one can recognize that the investigated SbSI/Sb_2S_3 heterojunctions are isotype. The p-type SbSI single crystals have been used for laser fabrication of the investigated SbSI/Sb_2S_3 heterostructures. Hence, it leads to conclusion that fabricated heterojunctions are p–p isotype. The p-type of amorphous Sb_2S_3 has been confirmed by electrical investigations of it.

Current flowing through SbSI/Sb_2S_3 heterojunction for reverse polarization depends linearly on applied voltage and is characterized by the absence of breakdown even for high voltages (Fig. 3). Activation energy $E_a = 0.417(22)$ eV of conductivity for reverse polarization has been determined.

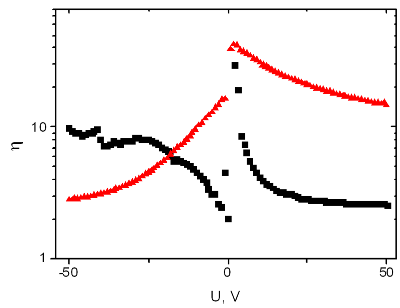

Fig. 4. Photosensitivity coefficients versus bias voltage for single SbSI/Sb_2S_3 (■) and double SbSI/Sb_2S_3/SbSI (▲) heterostructures ($\lambda = 652$ nm; illumination intensity $I_0 = 10^{22}$ photon/(m^2 s); $T = 313$ K).

Figure 4 presents typical photosensitivity (η), i.e. photocurrent to dark current ratio, of the fabricated heterostructures. In the case of single SbSI/Sb_2S_3 heterostructure (Fig. 1a) only the junction has been illuminated. During investigations of double SbSI/Sb_2S_3/SbSI (Fig. 1c) heterojunctions the Sb_2S_3 part of the heterostructure has been illuminated. For negligible bias voltages one can see the influence of photovoltaic effect on η open circuit voltage of an illuminated single SbSI/Sb_2S_3 junctions was about 2 V). For larger bias voltages photosensitivity of a single SbSI/Sb_2S_3 heterostructure is greater for reverse polarization than in the case of a typical photodiode. For forward polarization, photosensitivity of double SbSI/Sb_2S_3/SbSI heterostructure is higher than η of a single SbSI/Sb_2S_3 heterostructure. For reverse polarization, photosensitivity of SbSI/Sb_2S_3/SbSI heterostructure decreases with increasing the negative bias voltage. It is caused by the carriers traveling through two junctions oriented oppositely (Fig. 1c).

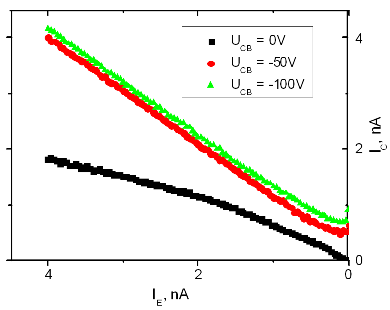

Fig. 5. Transient characteristics of Sb_2S_3/SbSI/Sb_2S_3 double heterostructure recorded for different U_{CB} voltages ($T = 303$ K).

Static electrical properties of Sb_2S_3/SbSI/Sb_2S_3 and SbSI/Sb_2S_3/SbSI heterostructures have been measured in a two-port network electrical circuit configurations OE, OB and OC appropriate for bipolar transistors. Typical transient characteristics in OB circuit have been presented in Fig. 5. Using such characteristics the common-base current gain factor $\alpha = I_C/I_E$ can be calculated. In the case of Sb_2S_3/SbSI/Sb_2S_3 heterostructure $\alpha \approx 0.5$ for not polarized collector-base junction and $\alpha \approx 1$ for polarized junction have been determined. These values are comparable with those of commercially available transistors. Analyzing characteristics presented in Fig. 5, one can notice that the ratios I_E/U_{CB} for double Sb_2S_3/SbSI/Sb_2S_3 heterostructure are significantly smaller than in the case of commercially available transistors. Simultaneously, the voltages applied to Sb_2S_3/SbSI/Sb_2S_3 heterostructures can be significantly higher than in the case of commercially available transistors. It is caused by the high resistance of fabricated heterostructures.

4. Conclusions

Electrical properties of CO_2 laser fabricated SbSI/Sb_2S_3, Sb_2S_3/SbSI/Sb_2S_3 and SbSI/Sb_2S_3/SbSI heterostructures have been determined for the first time. These structures are similar to diodes, transistors, as well as photodiodes and phototransistors under illumination. Current–voltage characteristics of the investigated structures have been fitted with theoretical formulae to determine the following types of the heterostructures: P–p SbSI/Sb_2S_3, p–P–p Sb_2S_3/SbSI/Sb_2S_3 and P–p–P SbSI/Sb_2S_3/SbSI. However, the relatively large ratios of recombination and diffusive currents in the junctions suppose the eventual inhomogeneity of them. Hence, the technology of laser preparation of single and multijunctions in SbSI single crystals needs additional investigations.

Hysteresis of the current–voltage characteristics of SbSI/Sb_2S_3 single junctions has been observed due to ferroelectric properties of SbSI below its Curie temperature ($T_c = 293$ K). Also the influence of coercive electric field on current–voltage characteristics of SbSI/Sb_2S_3 single junctions has been observed for $T < T_c$.

The fabricated double Sb_2S_3/SbSI/Sb_2S_3 heterostructures have high common-base current gain factor. Simultaneously, the ratios of I_E/U_{CB} for double Sb_2S_3/SbSI/Sb_2S_3 heterostructures are significantly smaller and the voltages applied to these heterostructures can be significantly higher than in the case of commercially available transistors. Electrical properties of the CO_2 laser fabricated SbSI/Sb_2S_3, Sb_2S_3/SbSI/Sb_2S_3 and SbSI/Sb_2S_3/SbSI heterostructures are photosensitive. It may lead to potentially new applications in electronics and optoelectronics.

Acknowledgments

One of the authors (B.T.) is a grant holder in "SWIFT" project POKL.08.02.01-24-005/10 co-funded by the European Union under the European Social Fund. The work was partially supported by NCN grant No. DEC-2011/01/B/ST5/06273.

References

[1] V.M. Fridkin, *Photoferroelectrics*, Springer-Verlag, New York 1979.

[2] V.M. Fridkin, *Ferroelectric Semiconductors*, Consultants Bureau, New York 1980.

[3] E.I. Gerzanich, V.M. Fridkin, *$A_5B_6C_7$ type Ferroelectrics*, Nauka, Moskva 1982 (in Russian).

[4] H. Akkus, A.M. Mamedov, *Centr. Europ. J. Phys.* **5**, 25 (2007).

[5] M. Nowak, P. Szperlich, Ł. Bober, J. Szala, G. Moskal, D. Stróż, *Ultrason. Sonochem.* **15**, 709 (2008).

[6] B. Toroń, M. Nowak, A. Grabowski, M. Kępińska, J. Szala, T. Rzychoń, *Proc. SPIE* **8497**, 84971K-1 (2012).

[7] S.M. Sze, K.K. Ng, *Physics of Semiconductor Devices*, Wiley, New Jersey 2007.

[8] K.E. Avdjian, *Mater. Res. Soc. Symp. Proc.* **692**, 491 (2002).

[9] H. Yang, H.M. Luo, H. Wang, I.O. Usov, N.A. Suvorova, M. Jain, D.M. Feldmann, P.C. Dowden, R.F. DePaula, Q.X. Jia, *Appl. Phys. Lett.* **92**, 1 (2008).

[10] Y. Watanabe, *Phys. Rev. B* **59**, 11257 (1999).

[11] E. Fatuzzo, G. Harbeke, W.J. Merz, R. Nitsche, H. Roetschi, W. Ruppel, *Phys. Rev.* **127**, 2036 (1962).

[12] T. Dam, L. Stourac, *Czech. J. Phys. B* **27**, 1409 (1977).